Sequential phase formation by ioninduced epitaxy in Feimplanted Si(001)

X. W. Lin, R. Maltez, M. Behar, Z. LilientalWeber, and J. Washburn

Citation: Journal of Applied Physics **78**, 4382 (1995); doi: 10.1063/1.359842
View online: http://dx.doi.org/10.1063/1.359842
View Table of Contents: http://scitation.aip.org/content/aip/journal/jap/78/7?ver=pdfcov
Published by the AIP Publishing

Sequential phase formation by ion-induced epitaxy in Fe-implanted Si(001)

X. W. Lin[a)]
Materials Science Division, Lawrence Berkeley Laboratory, University of California, Berkeley, California 94720

R. Maltez and M. Behar
Instituto de Fisica, UFRGS, 91501 Porto Alegre, Brazil

Z. Liliental-Weber and J. Washburn
Materials Science Division, Lawrence Berkeley Laboratory, University of California, Berkeley, California 94720

(Received 15 December 1994; accepted for publication 16 June 1995)

Ion-beam-induced epitaxial crystallization (IBIEC) of Fe-implanted Si(001) was studied by transmission electron microscopy and Rutherford backscattering spectrometry. For sufficiently high Fe doses, it was found that IBIEC at 320 °C results in sequential epitaxy of Fe silicide phases in Si, with a sequence of γ-$FeSi_2$, α-$FeSi_2$, and β-$FeSi_2$ with increasing Fe concentration along the implantation profile. The critical concentrations for the γ-α and α-β phase transitions were determined as ≈11 and 21 at. % Fe, respectively. The observed sequential phase formation can be correlated to the degree of lattice mismatch with the Si matrix and the stoichiometry of the silicide phases. © *1995 American Institute of Physics.*

I. INTRODUCTION

Regrowth of a preamorphized surface layer on Si crystals can be achieved either by thermally induced solid phase epitaxy (SPE) or by ion-beam-induced epitaxial crystallization (IBIEC). As opposed to thermal SPE,[1] IBIEC[2,3] is a nonequilibrium process, activated by ion irradiation that generates essentially point defects at the vicinity of the crystalline–amorphous (c–a) interface, and can occur in a relatively low temperature regime (200–400 °C) with a considerably smaller activation energy (≈0.3 eV). When used to crystallize an ion-implanted layer, IBIEC differs from SPE in many aspects, such as segregation[4,5] and precipitation[6–8] of the implanted solute atoms. In particular, if the precipitation involves compound formation, IBIEC may result in metastable phases, whereas SPE generally produces thermally stable ones. In the case of Fe-implanted Si, for instance, it has previously been reported that IBIEC at 320 °C can cause epitaxial growth of γ-$FeSi_2$ and α-$FeSi_2$; both are metastable relative to SPE-produced β-$FeSi_2$ which is the thermally stable disilicide below ≈950 °C.[6–8]

In this work, a new phenomenon of IBIEC is reported, i.e., sequential phase formation upon ion-induced regrowth of an Fe-implanted Si. The Fe–Si system was chosen in this study because there exist three Fe disilicide phases, γ-$FeSi_2$, α-$FeSi_2$, and β-$FeSi_2$, whose thermal stability (corresponding to enthalpy of formation) at room temperature increases in order of γ, α, and β,[8,9] as does the lattice mismatch with the Si matrix.[8] The variation in both thermal stability and lattice mismatch can have important consequences on nucleation and growth of an epitaxial phase. For sufficiently high Fe doses, it will be shown that ion-induced epitaxy at 320 °C proceeds by sequential phase formation of Fe silicides in the order shown above, as the c–a interface moves across the implantation profile. The results will be discussed in terms of the lattice mismatch with Si and the stoichiometry of the silicide phases.

II. EXPERIMENTAL

Si (001) wafers were first implanted at room temperature with 50 keV Fe^+ ions to different doses which were incrementally increased from 1×10^{16} to 8×10^{16} cm^{-2}, with a dose increment of 1×10^{16} cm^{-2}; the beam flux was 0.5 $\mu A\ cm^{-2}$. Channeling was avoided by tilting the wafer normal ≈7° away from the incident beam direction. It was found that the implant peak concentration c_p is proportional to the dose in the low dose range (each unit of 1×10^{16} cm^{-2} corresponds to c_p≈5 at. % Fe), but tends to saturate at c_p≈25 at. % Fe for high doses (≈8×10^{16} cm^{-2}). The implanted amorphous layer was crystallized at 320 °C by IBIEC, i.e., by irradiation with 380 keV Ne^+ ions to a fluence ranging from 4×10^{16} to 2×10^{17} cm^{-2}, depending on the Fe dose; the beam flux was 1 $\mu A\ cm^{-2}$. Prior to IBIEC, the as-implanted samples had not received any thermal treatment.

III. RESULTS

The crystallization process was monitored by Rutherford backscattering spectrometry combined with ion channeling (RBS/C). The RBS/C spectra (not shown here) indicated that the initial Fe implantation produces an a-Si layer ≈100 nm thick and that the subsequent Ne irradiation results in Si crystallization. The amount of crystallized Si depends on implanted Fe dose. For low Fe concentrations (c_p<≈10 at. %), a total Si crystallization can be achieved in the Ne fluence range given above, whereas for higher Fe concentrations, the IBIEC process cannot be completed, even for an extended Ne irradiation, leaving an a-Si surface layer, e.g., ≈25 nm thick for c_p≈25 at. % Fe. As for implanted Fe atoms, it was found that the Fe distribution is Gaussian-like, peaked at ≈38 nm below the surface with a width of ≈35 nm. IBIEC

[a)]Electronic mail: lin_x@RAVEN.SANJOSE.VLSI.COM

 0021-8979/95/78(7)/4382/4/$6.00

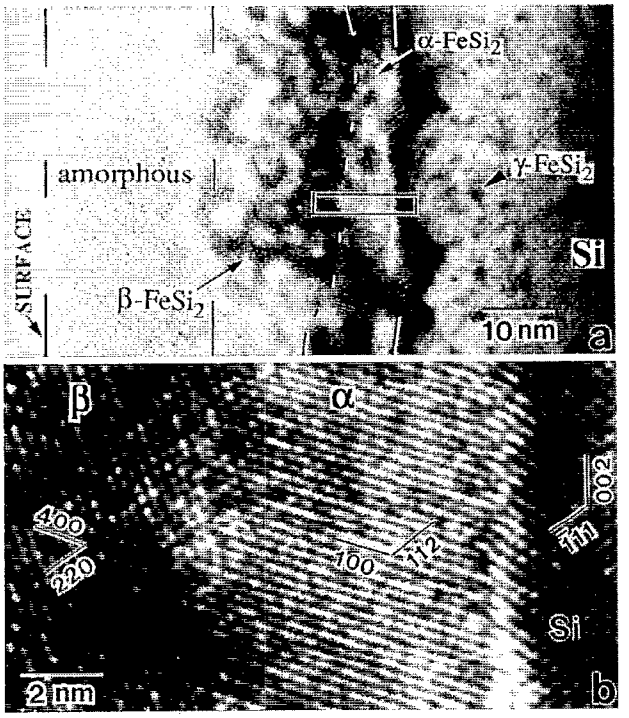

FIG. 1. (a) Cross-sectional TEM micrograph showing the phase distribution in a Si (001) sample implanted at room temperature with 6×10^{16} cm^{-2} of Fe atoms and subsequently crystallized by ion-beam-induced epitaxy at 320 °C. (b) High-resolution image of the rectangular area indicated in (a), showing the orientation relationship of α-$FeSi_2$ and β-$FeSi_2$ with respect to Si. The projection directions of lattice image are α-$FeSi_2$ [0$\bar{2}$1], β-$FeSi_2$[001], and Si[110].

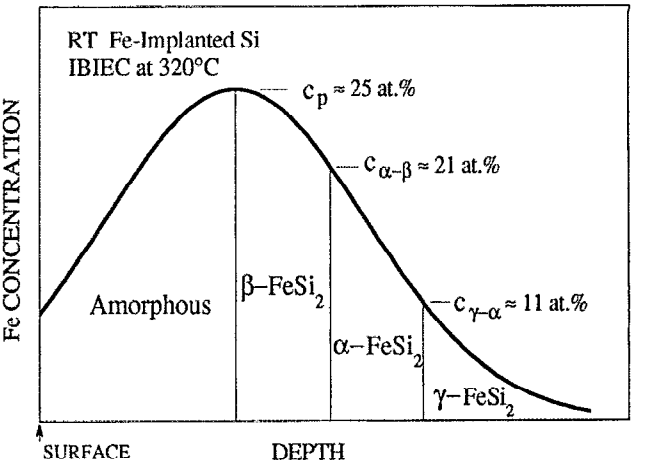

FIG. 2. Schematic diagram showing the sequence of silicide phase formation as a function of Fe concentration. The Fe implantation profile is approximated by a Gaussian distribution.

causes only a slight narrowing of the Fe peak; no peak shift was detected. In addition, some channeling was observed for low Fe doses ($c_p \lesssim 10$ at. %).

Structural characterization was performed, using transmission electron microscopy (TEM) on a JEOL 200CX high-resolution electron microscope. It was found that IBIEC induces epitaxial formation of $FeSi_2$ in Si, with the silicide phase depending on Fe concentration. Figure 1(a) shows a typical TEM image of a high dose (6×10^{16} cm^{-2}) sample, which displays a layered structure with a sequential phase formation along the crystallization direction. Similar structure was also observed for Fe doses in the range 4×10^{16}–8×10^{16} cm^{-2}, corresponding to c_p=21–25 at. % Fe. Since the implantation profile is Gaussian-like, the sequence of $FeSi_2$ phase formation shown in Fig. 1(a) can be associated with local Fe concentration, as schematically shown in Fig. 2. With increasing Fe concentration from the implantation profile tail, the silicide phase undergoes changes from γ-$FeSi_2$ to α-$FeSi_2$, and then to β-$FeSi_2$. The β-$FeSi_2$ layer continues to grow until it reaches a region around the implantation profile peak (i.e., the maximum Fe concentration), where IBIEC stops, leaving an amorphous surface layer ≈25 nm thick, in consistence with the RBS/C analysis. As shown in Fig. 1, the γ-$FeSi_2$ phase is formed as precipitates (≈1.5 nm diam) distributed over a region ≈20 nm wide, while α-$FeSi_2$ and β-$FeSi_2$ grow as continuous layers ≈10 and 15 nm thick, respectively, with a rough interface between them. Both the α-$FeSi_2$ and β-$FeSi_2$ layers consist of differently oriented crystal grains, with the lateral size much greater than the layer thickness. Notice that the interface between the α-$FeSi_2$ layer and the underlying region also appears rough and diffuse. It consists of areas in contact either with the Si substrate [as shown in Fig. 1(b)] or with γ-$FeSi_2$ precipitates (not shown here).

The concentration dependence of silicide phase formation suggests that there exist two critical concentrations $c_{\gamma\text{-}\alpha}$ and $c_{\alpha\text{-}\beta}$, corresponding to the transitions from γ-$FeSi_2$ to α-$FeSi_2$ and α-$FeSi_2$ to β-$FeSi_2$, respectively. These critical concentrations can be determined, by examining IBIEC-induced phase distribution as a function of the Fe dose. With increasing implant dose, the peak concentration at which α-$FeSi_2$ or β-$FeSi_2$ first appears corresponds to $c_{\gamma\text{-}\alpha}$ or $c_{\alpha\text{-}\beta}$, respectively. It was found that γ-$FeSi_2$ was the only phase formed for Fe doses below 2×10^{16} cm^{-2} ($c_p \approx 11$ at. %), while samples implanted with $2\times10^{16} \leq$ dose $< 4\times10^{16}$ cm^{-2} ($11 \leq c_p < 21$ at. %) showed the formation of α-$FeSi_2$ around the implantation profile peak, in addition to γ-$FeSi_2$ at the profile tail, a structure similar to our previous findings.[8] For doses $\geq 4\times10^{16}$ cm^{-2} ($c_p \approx 21$ at. %), the β-$FeSi_2$ phase emerged, in coexistence with γ-$FeSi_2$ and α-$FeSi_2$, as shown in Fig. 1(a). Based on these observations, one finds $c_{\gamma\text{-}\alpha} \approx 11$ at. % and $c_{\alpha\text{-}\beta} \approx 21$ at. %, as reported in Fig. 2. Since the dose increment used in this study was 1×10^{16} cm^{-2} (c_p=5 at. %), the uncertainty in the $c_{\gamma\text{-}\alpha}$ and $c_{\alpha\text{-}\beta}$ values is ±2.5 at. %.

The epitaxial relationships of the above silicide phases with respect to the Si matrix were readily revealed by high-resolution TEM, as well as by electron diffraction. For high Fe-dose samples, such as shown in Fig. 1, the typical orientation relationship can be written as

$$\mathrm{Si}[110]//\gamma[110]//\alpha[0\bar{2}1]//\beta[001]$$

and

$$\mathrm{Si}(\bar{1}11)//\gamma(\bar{1}11)//\alpha(112)//\beta(220).$$

This orientation relationship was found to hold, as the implant Fe dose decreases, along with successive disappearance of β-$FeSi_2$ and α-$FeSi_2$ that eventually leads to γ-$FeSi_2$ being

the only silicide in the system. Other orientations were also observed, but can be directly related to the above orientation relationship by twinning along the planes parallel to Si($\bar{1}$11), as described in previous studies.[7,8] Therefore, all silicide crystal grains can be considered as having an epitaxial relationship with the Si matrix, though a slight deviation from the above orientation relationship, i.e., a relative rotation between parallel planes by up to 3°, was observed for some α-$FeSi_2$ or β-$FeSi_2$ grains relative to Si.

IV. DISCUSSION

Epitaxial growth of the silicides indicates that the interface structure at the crystallization front plays an important role in phase formation during IBIEC. Among all the possible phases to be formed, the probability of finding a phase should increase, with decreasing lattice mismatch between this phase and the Si matrix, especially in the early stage of growth, where the interfacial energy counts significantly in the total free energy of the system. For samples implanted with $c_p < c_{\alpha\text{-}\beta}$, this mechanism has previously been proposed to explain why the γ phase is the first to form during IBIEC and why α-$FeSi_2$ is subsequently formed instead of β-$FeSi_2$, even though the β phase is thermally more stable.[8] The answer lay in the fact that the α phase is better lattice matched with Si than the β phase, while the γ phase is best matched with Si among the three phases.

In addition to the lattice mismatch argument, the stoichiometry of the silicides also favors the α phase over the β phase. From the Fe–Si phase diagram, while β-$FeSi_2$ is a stoichiometric phase, the α phase can exist with a large number of Fe vacancies (up to ≈20 at. %).[10,11] Therefore, if the composition of an Fe–Si system is considerably less than the $FeSi_2$ stoichiometry (i.e., 33.3 at. % Fe), the formation of α-$FeSi_2$ should be preferred over β-$FeSi_2$, since the α phase can tolerate a relatively high Fe deficiency. However, if the Fe concentration approaches the $FeSi_2$ stoichiometry, the formation of β-$FeSi_2$ should be expected. This composition dependence of phase formation suggests that an α-β phase transition is likely to occur if the system exhibits a concentration gradient in a certain composition range, such as the case for Fe-implanted Si samples with high Fe doses ($c_p > c_{\alpha\text{-}\beta}$).

Following the above line of discussion, a plausible explanation can be proposed to account for the observation that IBIEC stops around the maximum Fe concentration (Figs. 1 and 2). Suppose that ion-induced crystallization could proceed beyond the implant peak region, a progressive decrease of Fe concentration at the c-a interface is expected, as the crystal growth front moves toward the surface. From the stoichiometric point of view, if β-$FeSi_2$ is formed in the implant peak region, the decrease in Fe concentration would favor a β-$FeSi_2$ to α-$FeSi_2$ phase transition, inversing the previous order of silicide phase formation. Two factors, however, may hinder the α-$FeSi_2$ epitaxy on β-$FeSi_2$. First, since α-$FeSi_2$ is a high-temperature phase and unstable against β-$FeSi_2$ at the growth temperature, there is no thermodynamic driving force for the β-α phase transition to occur. Second, the α-$FeSi_2$ epitaxy on β-$FeSi_2$ would involve a minimum lattice mismatch of ≈2.2%,[8] as compared with a ≈0.7% mismatch[8] for α-$FeSi_2$ grown on either Si or γ-$FeSi_2$ during the first part of IBIEC (see, e.g., Fig. 1). In other words, the lattice mismatch does not favor the β-α phase transition either. Because of these two factors, it does not seem surprising that IBIEC cannot go beyond the implant peak region.

One question remains to be answered. That is, since the peak concentration in high Fe dose samples is c_p≈25 at. % Fe, considerably smaller than the stoichiometric value 33.3 at. % Fe, how can β-$FeSi_2$ be formed in such Fe deficient samples? It is possible that ion-beam-enhanced diffusion occurred during IBIEC, resulting in an increase in local Fe concentration.

As stated above, IBIEC is a nonequilibrium process, which can produce metastable phases and structures. Indeed, by annealing high Fe-dose samples, such as shown in Fig. 1, at 800 °C for 0.5 h, we found that both the γ and α phases transform into the β phase. For a longer anneal (≈8 h), the silicide layer was found to disintegrate into laterally separated large precipitates.

V. CONCLUSION

This work demonstrates that ion-beam-induced crystallization of Fe-implanted Si involves epitaxial growth of $FeSi_2$ silicides in the phase sequence of γ, α, and β, with increasing Fe concentration along the implantation profile. Thus, IBIEC can be used as a novel way to produce heteroepitaxial structures, though the interface quality (e.g., flatness) needs further improvement for them to be of practical use. The observed results can be accounted for, in terms of the lattice mismatch with the Si matrix and the stoichiometry of these silicide phases. Bulk thermodynamic properties (e.g., enthalpy of formation) of the silicides does not seem to play the dominant role during the ion-induced epitaxial phase formation.

ACKNOWLEDGMENTS

This work was supported by the Director, Office of Energy Research, Office of Basic Energy Sciences, Materials Science Division of the U.S. Department of Energy under Contract No. DE-AC03-76SF00098. The use of the facilities of the National Center for Electron Microscopy is acknowledged. The authors are grateful to Dr. H. Bernas for valuable discussions. They also wish to thank W. Swider for TEM sample preparation.

[1] G. L. Olson and J. A. Roth, Mater. Sci. Rep. **3**, 1 (1988).
[2] J. M. Poate, D. C. Jacobson, F. Priolo, and M. O. Thompson, Mater. Res. Soc. Symp. Proc. **128**, 533 (1989).
[3] F. Priolo and E. Rimini, Mater. Sci. Rep. **5**, 319 (1990).
[4] J. M. Poate, J. Linnros, F. Priolo, D. C. Jacobson, J. L. Batstone, and M. O. Thompson, Phys. Rev. Lett. **60**, 1322 (1988).
[5] F. Priolo, J. L. Bastone, J. M. Poate, J. Linnros, D. C. Jacobson, and M. O. Thompson, Appl. Phys. Lett. **52**, 1043 (1988).
[6] J. Desimoni, H. Bernas, M. Behar, X. W. Lin, J. Washburn, and Z. Liliental-Weber, Appl. Phys. Lett. **62**, 306 (1993).
[7] X. W. Lin, M. Behar, J. Desimoni, H. Bernas, W. Swider, Z. Liliental-Weber, and J. Wahburn, Mater. Res. Soc. Symp. Proc. **279**, 535 (1993); X. W. Lin, J. Desimoni, H. Bernas, Z. Liliental-Weber, and J. Washburn, *ibid.* **320**, 97 (1994).

[8] X. W. Lin, M. Behar, J. Desimoni, H. Bernas, J. Washburn, and Z. Liliental-Weber, Appl. Phys. Lett. **63**, 105 (1993), and references therein.
[9] X. W. Lin, J. Washburn, Z. Liliental-Weber, and H. Bernas, J. Appl. Phys. **75**, 4686 (1994).
[10] T. B. Massalski, *Binary Alloy Phase Diagrams* (American Society for Metals, Metals Park, OH, 1986).
[11] K. Radermacher, S. Mantl, Ch. Dieker, and H. Lüth, Appl. Phys. Lett. **59**, 2145 (1991).